



ELSEVIER

Physica B 305 (2001) 83–89

PHYSICA B

www.elsevier.com/locate/physb

# Local structure of random $\text{In}_x\text{Ga}_{1-x}\text{As}$ alloys by full-profile fitting of atomic pair distribution functions

V. Petkov\*, S.J.L. Billinge

*Department of Physics and Astronomy and Center for Fundamental Materials Research, Michigan State University,  
East Lansing, MI 48823, USA*

Received 7 March 2001

## Abstract

The local structure of random  $\text{In}_x\text{Ga}_{1-x}\text{As}$  alloys has been refined by fitting experimental high-resolution atomic pair distribution functions with the 8-atom unit cell of the zinc-blende lattice. Both metal and As atoms have been allowed to move off their ideal positions and so the local structural disorder due to the presence of two distinct bond lengths, Ga–As and In–As, has been quantified. It has been found that most of the disorder is accommodated by the As sublattice but the disorder on metal sites is important too. This new experimental information has been incorporated into a larger, statistically representative, model of  $\text{In}_{0.5}\text{Ga}_{0.5}\text{As}$  structure using widely available crystallographic software. © 2001 Elsevier Science B.V. All rights reserved.

*PACS:* 61.66.Dk; 61.43.Dq

*Keywords:*  $\text{In}_x\text{Ga}_{1-x}\text{As}$ ; Local structure; Atomic pair distribution

## 1. Introduction

Ternary semiconductor alloys, including  $\text{In}_x\text{Ga}_{1-x}\text{As}$ , have been thoroughly studied because of their importance in applications such as electronic and optical devices [1,2]. Special attention has been paid to the structure at atomic scale since it is well known that the atomic arrangement determines most of the physical properties and technological characteristics of materials. It has been found that  $\text{In}_x\text{Ga}_{1-x}\text{As}$  alloys crystallize in the cubic zinc-blende structure and their lattice parameters interpolate linearly between those of

the end members, GaAs and InAs. Since this behaviour is consistent with the so-called Vegard's law, the atomic arrangement of  $\text{In}_x\text{Ga}_{1-x}\text{As}$  alloys is often approximated with a virtual zinc-blende type lattice where all bond lengths are taking equal, compositionally averaged, values and the bond angles remain unperturbed from the ideal tetrahedral ones. However, XAFS experiments [3] have shown that Ga–As and In–As bonds indeed remain close to their natural lengths of 2.43 and 2.61 Å, respectively. This finding is close to the so-called Pauling limit [4] and implies that the zinc-blende lattice of  $\text{In}_x\text{Ga}_{1-x}\text{As}$  is distorted locally to accommodate the two distinct Ga–As and In–As bonds lengths present. XAFS results inspired further research and several models for the distorted structure of  $\text{In}_x\text{Ga}_{1-x}\text{As}$  alloys have

\*Corresponding author. Tel.: +1-517-353-5288; fax: +1-517-353-4500.

*E-mail address:* petkov@pa.msu.edu (V. Petkov).

been proposed [5–7]. The models have been obtained by relaxing supercells based on the zincblende lattice using Keating or Kirkwood interatomic potentials. They have been found to reproduce the experimental data well and thus are a good starting point for any further calculations requiring more realistic knowledge of the alloy's structure. The success of this approach, however, relies on the presence of suitable interatomic potentials which may not be the case with many materials of scientific and technological importance. It is obviously important to have a technique allowing the structure of locally disordered materials to be studied on the basis of the experimental data alone without recourse to any potential-based approximations. In the present paper we show that detailed structural information about crystalline materials with intrinsic disorder, such as random  $\text{In}_x\text{Ga}_{1-x}\text{As}$  alloys, can be extracted by a profile fitting of experimental atomic pair distribution functions (PDF) in a manner very similar to that employed by the Rietveld technique [8]. Moreover, we show that structure models incorporating this information can be easily built using widely available crystallographic software. This novel approach becomes possible owing to the advent of powerful X-ray and neutron sources allowing accurate high-resolution PDFs to be obtained [9–11].

## 2. Experimental and computational details

### 2.1. High-energy X-ray diffraction experiments

The reduced atomic PDF,  $G(r)$ , is the instantaneous atomic number density–density correlation function which describes the atomic arrangement in materials [12,13]. It is the sine Fourier transform of the experimentally observable structure factor,  $S(Q)$ , given by

$$G(r) = 4\pi r [\rho(r) - \rho_0] \\ = (2/\pi) \int_{Q=0}^{Q_{\max}} F(Q) \sin(Qr) dQ, \quad (1)$$

with  $F(Q) = Q[S(Q) - 1]$ ,  $Q$  being the magnitude of the wave vector, and  $\rho(r)$  and  $\rho_0$  the local and

average atomic number density, respectively. The total structure factor,  $S(Q)$ , is defined by

$$S(Q) = 1 + \left[ I^{\text{el.}}(Q) - \sum c_i f_i^2(Q) \right] / \left[ \sum c_i f_i(Q) \right]^2, \quad (2)$$

where  $I^{\text{el.}}$  is the elastic part of the total diffraction spectrum;  $c_i$  and  $f_i(Q)$  are the atomic concentration and usual scattering factor of the atomic species of type  $i$ , respectively. An important characteristic of the PDF is to be noted: Since  $S(Q)$  includes both Bragg peaks and the diffuse component(s) of the diffraction spectrum, its Fourier associate, the PDF reflects both the *local* and *average* atomic structure of materials. In addition, the PDF is particularly sensitive to the atomic short-range ordering since the scattered intensities are weighted by their wave vectors  $Q$  (see the kernel of the integral of Eq. (1)). This makes the PDF a structural quantity very suitable in characterizing materials where deviations from the average structure are present.

Very high real space resolution is required to reveal the individual bond lengths and the associated local structural distortions in  $\text{In}_x\text{Ga}_{1-x}\text{As}$  alloys. We achieved it by carrying out diffraction experiments using high energy X-rays delivered by the A2 24 pole wiggler of the Cornell High Energy Synchrotron Source. The experiment was described in recent papers [7,9]; a few details are reproduced here for clarity. Six powder samples of  $\text{In}_x\text{Ga}_{1-x}\text{As}$  with  $x = 0.0, 0.17, 0.33, 0.5, 0.83, 1.0$ , were measured with the use of X-rays of energy 60 keV at 10 K. Low temperature was used to minimize thermal vibrations in the samples and, hence increase the sensitivity to local structural distortions. Scattered radiation was collected with an intrinsic germanium detector connected to a multichannel analyzer. The data were normalized for flux, corrected for detector dead time, background scattering and absorption and reduced to the total structure factor,  $S(Q)$ , using the program RAD [14]. Experimental reduced structure factors,  $F(Q) = Q[S(Q) - 1]$ , are shown in Fig. 1 and the corresponding atomic PDFs—in Fig. 2.

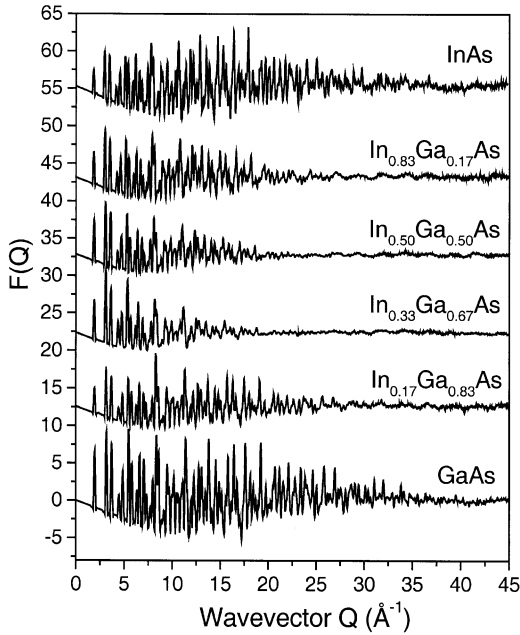


Fig. 1. Experimental structure factors,  $F(Q)$ , for  $\text{In}_x\text{Ga}_{1-x}\text{As}$  alloys.

### 2.2. Full-profile fitting of the experimental PDFs

The atomic PDF technique has been the approach of choice in characterizing glasses and liquids for a long time [12,13]. Its application to crystalline materials with intrinsic disorder is relatively recent [10,11] and may be viewed as a real-space analogue of Rietveld refinement of powder diffraction spectra [15]. The PDF full-profile fitting starts with the selection of a unit cell that is consistent with the average crystal structure. A model PDF is calculated and compared with the experimental one. Structural parameters such as unit cell constants, atomic positions and thermal factors are then varied in a way to improve the agreement between the calculated and experimental PDFs. The refinement process is terminated when all important details in the experimental PDF are well reproduced. The usual goodness-of-fit indicator,  $R_{\text{wp}}$ ,

$$R_{\text{wp}} = \left\{ \frac{\sum w_i (G_i^{\text{exp.}} - G_i^{\text{calc.}})^2}{\sum W_i (G_i^{\text{exp.}})^2} \right\}^{1/2} \quad (3)$$

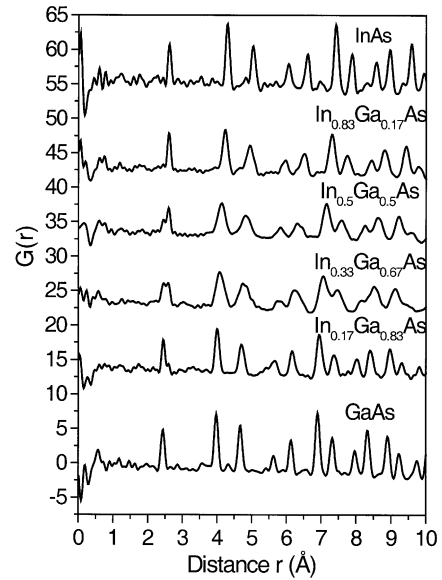


Fig. 2. Experimental atomic pair distribution functions,  $G(r)$ , for  $\text{In}_x\text{Ga}_{1-x}\text{As}$  alloys.

is used to estimate the success of the structure refinement. Here  $G^{\text{exp.}}$  and  $G^{\text{calc.}}$  are the experimental and calculated PDFs, respectively, and  $w_i$  are weighting factors reflecting the statistical quality of the individual data points. The quality of the present PDFs was estimated and the individual  $w_i$  determined with the help of the program IFO [16]. The program employs statistical procedures based on the maximum entropy method to estimate the experimental uncertainty in each PDF data point; the reciprocal of this uncertainty was used as  $w_i$ . One point deserves to be mentioned here: The agreement factor  $R_{\text{wp}}$  introduced by Eq. (3) may appear high when compared to agreement factors reported with single crystal and Rietveld refinements. This does not indicate an inferior structure refinement but merely reflects the fact that the PDF function being fit is not the one fit in a Rietveld refinement and is a much more sensitive quantity. The sensitivity comes from the extra  $r/Q$  “pre-factors” in the Fourier couple  $G(r) = 4\pi r[\rho(r) - \rho_0]/Q[S(Q) - 1]$  (see Eq. (1)). Note, Rietveld refinements rely on the raw diffraction spectrum, a quantity analogous to  $S(Q)$ . An agreement factor that is closer to the one used with the Rietveld

refinements can be computed by dropping the “pre-factor”  $r$  and using the PDF  $g(r) = \rho(r)/\rho_0$  and not the PDF  $G(r)$  in Eq. (3). For the sake of clarity, we report two  $R_{\text{wp},s}$  in the present paper: one computed with the PDF  $G(r)$  and the other with the PDF  $g(r)$ .

The present structure refinements were based on the 8-atom unit cell of the zinc-blende structure because this is the atomic configuration of minimal complexity that fully explains the Bragg diffraction patterns of  $\text{In}_x\text{Ga}_{1-x}\text{As}$  alloys [17]. In accordance with the experiment the overall symmetry of the unit cell was kept cubic during the refinements and so only the length of the cell’s edge could be refined. In this simple unit cell, it is impossible to sample all chemical environments of As occurring in the random alloys of the concentration considered. To avoid the creation of preferential chemical ordering the four metal sites in the unit cell were populated with one atomic type having the average scattering power of  $x\text{In} + (1-x)\text{Ga}$  atoms. The presence of two distinct bond lengths in the alloys, however, required that the 8 atoms in the unit cell occupy specific sites. It was achieved by letting the atoms move off their ideal positions. For simplicity, all four As atoms were constrained to be displaced by the same amount as each other. The metal atoms were likewise constrained to have the same displacement amplitude, but the metal site displacements were independent of the As sublattice displacements. The directions of the discrete displacements of both As and metal atoms were constrained to be along  $\langle 111 \rangle$  directions in the cubic lattice, i.e. along the shortest path connecting two neighbouring atoms in the cubic unit cell. Thus, for instance, the As atom occupying the ideal site  $(0, 0, 0)$  was allowed to move to  $(\pm\varepsilon, \pm\varepsilon, \pm\varepsilon)$  and the metal atom at  $(1/4, 1/4, 1/4)$  to  $(1/4 \pm \delta, 1/4 \pm \delta, 1/4 \pm \delta)$ . The highly anisotropic,  $\langle 111 \rangle$  character of the individual atomic displacements follows from simple crystallographic considerations [7,18] and has been predicted by several potential-based models [5,7,19]. These models predict a small displacement in  $\langle 100 \rangle$  direction as well. We obtained adequate fit to the data without explicitly accounting for it. It is not a surprise since the  $\langle 100 \rangle$  displacements have been shown to be significant at concentra-

tions close to  $x = 0.5$  only (see Fig. 9 in Ref. [7]). It should be pointed out that the splitting of the first peak in the experimental PDFs is very sensitive to the discrete displacements. This splitting is indeed what determined the amplitudes and directions of the displacements of As and metal atoms in the refined unit cell. In addition to the anisotropic, discrete atomic displacements, isotropic atomic mean-square displacements (thermal factors),  $\langle u^2 \rangle$ , of As and metal atoms were refined. In comparing with experiment, the model PDF was convoluted with a Sine function to account for the truncation of the experimental data at  $Q_{\text{max}}$ . All refinements were done with the help of the program PDFFIT [20]. A comparison between the experimental and best-fit-achieved PDFs is shown in Figs. 3 and 4.

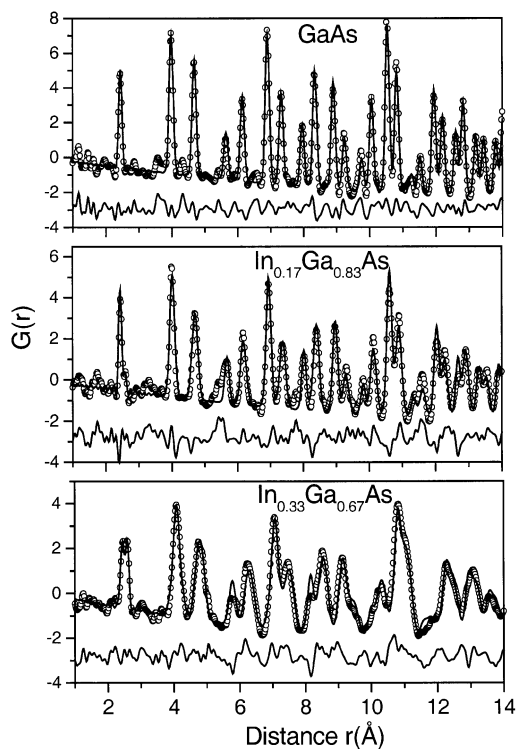


Fig. 3. Experimental (symbols) and fitted (solid line) PDFs for  $\text{In}_x\text{Ga}_{1-x}\text{As}$  alloys ( $x = 0.0.17, 0.33$ ). The residual difference between the fit and the experimental data is given in the lower part.

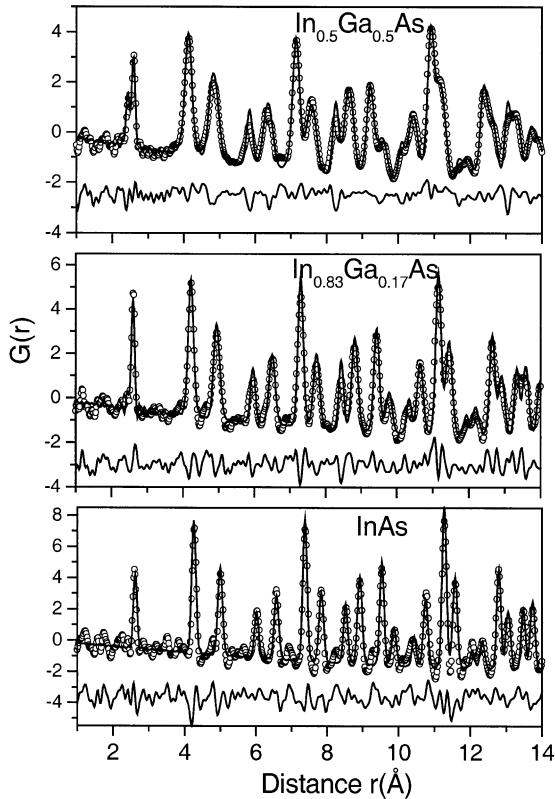


Fig. 4. Experimental (symbols) and fitted (solid line) PDFs for  $\text{In}_x\text{Ga}_{1-x}\text{As}$  alloys ( $x = 0.5, 0.83, 1.0$ ). The residual difference between the fit and the experimental data is given in the lower part.

### 3. Results

Bragg peaks are immediately evident in the structure factors of InAs and GaAs up to  $Q \sim 35 \text{ \AA}^{-1}$ . This shows that the end members exhibit little positional disorder at the atomic scale. The lack of structural disorder is also demonstrated by the fact that all peaks in the corresponding PDFs are quite sharp. The Bragg peaks disappear at much lower wave vectors in the  $F(Q)$ 's of  $\text{In}_x\text{Ga}_{1-x}\text{As}$  alloys, also shown in Fig. 1. At high- $Q$  values, only oscillating diffuse scattering is present. The presence of sharp Bragg peaks at low wave vectors implies that the alloys are still long-range ordered. The lack of Bragg peaks at higher wave vectors, however, shows that the alloys have significant local disorder. The disorder

is due to the mismatch of Ga–As and In–As bond lengths seen as a first split peak in the corresponding PDFs shown in Fig. 2. This peak is, however, the only one which stays sharp in the experimental PDFs. All peaks positioned at higher  $r$  values are significantly broadened in the alloys due to local atomic displacements. The broadening is intrinsic and not due to any experimental limitations since it is not present in the PDFs of the end members exhibiting no structural disorder.

With only three variable parameters, the lattice constant and the thermal factors of metal and As atoms, an almost perfect fit to the experimental PDFs of the end members, GaAs and InAs, is achieved as one can see in Figs. 3 and 4. The oscillations of the difference curve are nowhere greater than the noise in the data seen at very low values of  $r$ . The value of the goodness-of-fit indicator,  $R_{\text{wp}}$ , is about 20%, and it is only about 8% when the PDF  $g(r)$  and not the PDF  $G(r)$  are compared to each other. Both the flat difference curve and the relatively low values of the goodness-of-fit indicators achieved show that the fits are successful. They confirm the finding of single crystal experiments [17] that metal and As atoms in GaAs and InAs are arranged on the vertices of a perfect zinc-blende type lattice. Fits of the same quality were obtained with the structure refinement of the alloys. Here the splitting of the first peak and the broadening of the subsequent peaks in the experimental PDFs required that both metal and As atoms are displaced from their positions in the ideal lattice and the temperature factors of both As and metal atoms are enlarged. The refined lattice parameters, amplitudes of the discrete atomic displacements,  $\varepsilon$  and  $\delta$ , and thermal factors are given in Fig. 5.

### 4. Discussion

In agreement with all conventional diffraction experiments [17] the present results showed that the average structure of  $\text{In}_x\text{Ga}_{1-x}\text{As}$  alloys is well described with the 8-atom cubic unit cell of the zinc-blende lattice with the lattice constant varies linearly with composition  $x$  (see Fig. 5, the upper panel). In addition, the profile fitting of atomic

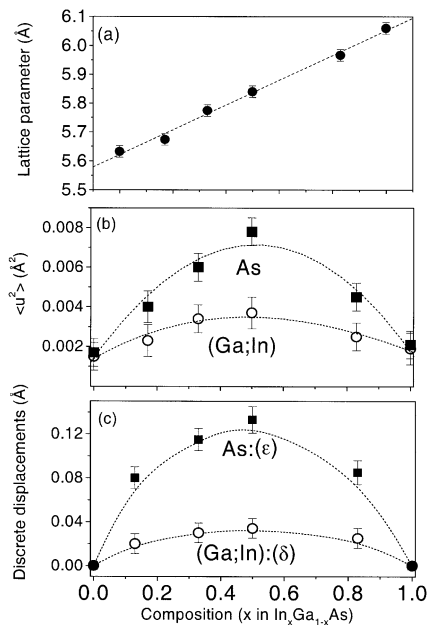


Fig. 5. Lattice constants (a), mean-square (b) and discrete (c) displacements of metal ( $\delta$ ) and As ( $\epsilon$ ) atoms from their positions in an ideal zinc-blende lattice as extracted from 8-atom unit cell refinements guided by the experimental PDFs. The results of a linear fit to the lattice constants and a second order polynomial fit to the atomic displacements are also shown (dashed curves).

PDFs yields information beyond the well-known average crystal structure revealing information about exactly how the zinc-blende lattice distorts locally to accommodate the distinct Ga–As and In–As bond lengths. The bond-length difference is  $\sim 0.15(1)\text{Å}$  in the alloys (see Fig. 3 in Ref. [9]). This difference forces all atoms off their ideal positions with the displacement of As atoms,  $\epsilon$ , is more pronounced than that of the metal atoms,  $\delta$ . The appearance of discrete, highly anisotropic atomic displacement is, however, not the only way in which the zinc-blende lattice responds to the bond-length mismatch. The lattice as a whole relaxes as the extra increase in the mean-square atomic displacements,  $\langle u^2 \rangle$ , indicates. Again most of the relaxation occurs on the As sublattice and that on the metal sublattice although smaller, is always significant. Interestingly, both the discrete and mean-square atomic displacement can be well fit with a polynomial of a second order. The presence of a quadratic dependence of the degree

of local structural disorder on the concentration,  $x$ , peaking at  $x = 0.5$  has been predicted by several potential-based models [5–7,9].

It has been shown that electronic and other physical properties of semiconductors are highly sensitive to details of the atomic ordering, including small changes in atomic positions, and that structure models reflecting these details are important for predicting the material's properties [21]. The refined 8-atom unit cells of  $\text{In}_x\text{Ga}_{1-x}\text{As}$  describes the details in the atomic ordering well and so could be a good starting point for building such structure models. To demonstrate the feasibility of the approach we show how a 512-atom model of the structure of  $\text{In}_{0.5}\text{Ga}_{0.5}\text{As}$  can be built using widely available crystallographic software, namely the program DISCUS [22]. First, a configuration of 512 atoms having the ideal zinc-blende structure is created. Then the metal sublattice is populated with Ga and In atoms at random. Each metal and As atom is then moved off its ideal position in  $\langle 111 \rangle$  direction with the respective amplitude of the displacement equals the one shown in Fig. 5. The choice of which of the eight possible  $\langle 111 \rangle$  directions is determined by the particular chemical environment. Finally, all atomic sites are relaxed with the  $\langle u^2 \rangle$  values also shown in Fig. 5. A variety of PDFs calculated on the basis of this 512-atom configuration are shown in Fig. 6. As can be seen the calculated and experimental total PDFs are in very good agreement. The calculated In-differential PDF is also in good agreement with the experimental one reported elsewhere [23]. All calculated PDFs agree well with those derived from another 512-atom model based on the Kirkwood potential [6]. Therefore, the present model may be considered to describe the local structure of  $\text{In}_{0.5}\text{Ga}_{0.5}\text{As}$  well. It also well represents all possible environments of As atoms and has the extra advantage of not being based on any theoretical assumptions.

## 5. Conclusions

Details of the atomic arrangement in crystalline materials with intrinsic disorder can be obtained by profile fitting of experimental high-resolution

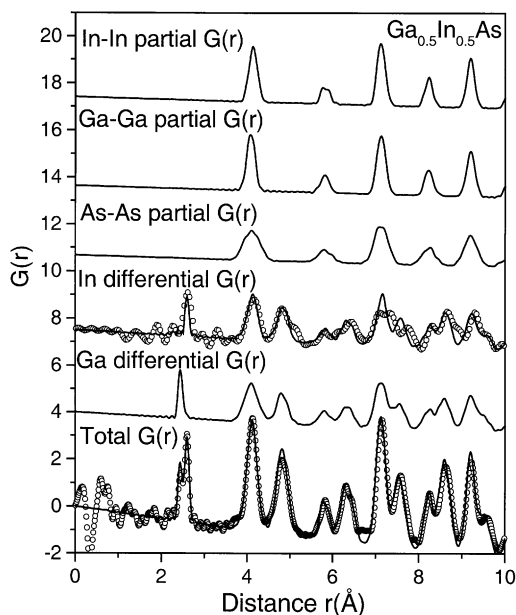


Fig. 6. Experimental (symbols) and model (solid line) atomic PDFs for  $\text{In}_{0.5}\text{Ga}_{0.5}\text{As}$ . The model PDFs are based on a distorted zinc-blende structure type configuration of 512 atoms exhibiting the discrete and mean-square displacements shown in Fig. 5.

PDFs. In particular, the present structure refinements of the 8-atom unit cell of  $\text{In}_x\text{Ga}_{1-x}\text{As}$  show that the arsenic sublattice contains most of structural disorder in the alloys. Significant disorder is also present on the metal sublattice. It is also shown that the refined structure parameters can be incorporated into structure models of bigger size using available crystallographic software. Thus a basis for more precise calculations of properties of crystalline material with intrinsic disorder can be created without any recourse to potential-based approximations.

### Acknowledgements

We would like to acknowledge the help of I.-K. Jeong and S. Kycia in collecting the data. The

work was supported by the US-DOE through grant DE-FG02-97ER45651. CHESS is operated by NSF through grant DMR97-13424.

### References

- [1] J.C. Wooley, in: R.K. Willardson, H.L. Goering (Eds.), *Compound Semiconductors*, Reinhold, New York, 1962.
- [2] V. Narayanamuri, *Science* 235 (1987) 1023.
- [3] J.C. Mikkelsen, J.B. Boyce, *Phys. Rev. Lett.* 49 (1982) 1412.
- [4] L. Pauling, *The Nature of the Chemical Bond*, Cornell University Press, New York, 1967.
- [5] M. Schabel, J.L. Martins, *Phys. Rev. B* 43 (1991) 11873.
- [6] J. Chung, M. Thorpe, *Phys. Rev. B* 59 (1999) 4807.
- [7] I.-K. Jeong, F.M. Jacobs, V. Petkov, S.J.L. Billinge, S. Kycia, *Phys. Rev. B* 63 (2001) 205202.
- [8] H. Rietveld, *J. Appl. Crystallogr.* 2 (1969) 65.
- [9] V. Petkov, I.-K. Jeong, J.S. Chung, M.F. Thorpe, S. Kycia, S.J.L. Billinge, *Phys. Rev. Lett.* 83 (1999) 4089.
- [10] T. Egami, *Mater. Trans.* 31 (1990) 163.
- [11] T. Egami, in: S.J.L. Billinge, M. Thorpe (Eds.), *Local Structure from Diffraction*, Plenum, New York, 1998, p. 1.
- [12] B.E. Warren, *X-ray Diffraction Procedures*, Dover, New York, 1990.
- [13] C.N.J. Wagner, *J. Non-Cryst. Solids* 31 (1978) 1.
- [14] V. Petkov, *J. Appl. Crystallogr.* 22 (1989) 387.
- [15] S.J.L. Billinge, in: S.J.L. Billinge, M. Thorpe (Eds.), *Local Structure from Diffraction*, Plenum Press, New York, 1998, p. 137.
- [16] V. Petkov, R. Danev, *J. Appl. Crystallogr.* 31 (1998) 609.
- [17] R.W.G. Wyckoff, *Crystal Structures*, Wiley, New York, 1967.
- [18] A. Balzarotti, N. Motta, A. Kisiel, M. Zimnal-Starnawska, M.T. Czyzyk, M. Podgorni, *Phys. Rev. B* 31 (1985) 7586.
- [19] A. Silverman, A. Zunger, R. Calish, J. Adler, *Europhys. Lett.* 31 (1995) 373.
- [20] Th. Proffen, S.J.L. Billinge, *J. Appl. Crystallogr.* 32 (1999) 572.
- [21] A. Zunger, S.-H. Wei, L.G. Ferreira, J.E. Bernard, *Phys. Rev. Lett.* 65 (1990) 353.
- [22] Th. Proffen, R.B. Neder, *J. Appl. Crystallogr.* 30 (1997) 171.
- [23] V. Petkov, I.-K. Jeong, F. Mohiuddin-Jacobs, Th. Proffen, S.J.L. Billinge, W. Dmowski, *J. Appl. Phys.* 88 (2000) 665.